

# Streamline Curvature Effects on Turbulent Boundary Layers

D.C. Wilcox\* and T.L. Chambers†  
*DCW Industries, Inc., Sherman Oaks, Calif.*

A theoretical tool has been developed for predicting, in a nonempirical manner, effects of streamline curvature and coordinate-system rotation on turbulent boundary layers. Specifically, the second-order closure scheme developed by Wilcox and Traci has been generalized for curved streamline flow and for flow in a rotating coordinate system. A straightforward, physically based argument shows that curvature/rotation primarily affects the turbulent mixing energy; the argument yields suitable curvature/rotation terms which are added to the mixing-energy equation. Singular-perturbation solutions valid in the wall layer of 1) a curved-wall boundary layer and 2) fully developed rotating channel flow demonstrate that, with the curvature/rotation terms, the model predicts the curved-wall and the rotating-coordinate-system laws of the wall. Results of numerical computations of curved-wall boundary layers and of rotating channel flow show that curvature/rotation effects can be computed accurately with second-order closure.

## I. Introduction

EFFECTS of streamline curvature on turbulent boundary layers have been under investigation for about forty years. However, as noted by Bradshaw,<sup>1</sup> experimentally observed effects of streamline curvature have had a "curious lack of impact" on engineering calculation methods. With the advent of more and more sophisticated turbulent-boundary-layer calculation methods in recent years, analytical prediction of streamline-curvature effects on turbulent boundary layers has received increasing attention for three key reasons; namely, 1) streamline curvature produces unexpectedly large changes in boundary-layer properties, 2) many practical aerodynamic surfaces are sufficiently curved to produce significant curvature effects, and 3) these effects are either unaccounted for or inadequately represented by current analytical tools.

Typical examples of the profound influence of streamline curvature on turbulent-boundary-layer development are demonstrated by Meroney and Bradshaw<sup>2</sup> and by Thomann.<sup>3</sup> In the case of incompressible, constant-pressure flow over both convex and concave walls, Meroney and Bradshaw find that for a radius of curvature,  $R$ , a hundred times the boundary-layer thickness,  $\delta$ , skin friction differs from its corresponding plane-wall value by as much as 10% while boundary-layer thickness is halved on the convex surface. (By contrast, laminar skin friction changes by about 1% for  $\delta/R = 0.01$ .) Similar results have been observed by Thomann for supersonic boundary layers; for constant pressure flow over curved surfaces with  $\delta/R \sim 0.02$ , heat transfer changes by nearly 20%.

In his review article, Bradshaw expresses pessimism regarding development of a universally applicable turbulent-boundary-layer computation method which includes effects of streamline curvature which are, in Bradshaw's terminology, a result of "extra rates of strain." He goes so far as to state that, "there is no immediate prospect of a calculational method that will naturally predict all the effects of extra rates of strain, even in thin shear layers." In Bradshaw's terminology, an unnatural prediction presumably is made by using an existing turbulence theory with an empirically devised curvature modification. Unnatural predictive tools are not without value, and there have been recent at-

tempts to incorporate effects of curvature into mixing-length models. Bradshaw,<sup>1</sup> for example, introduces a relaxation concept to account for curvature, while Eide and Johnston<sup>4</sup> devise empirical modifications to the mixing length. Both methods and other similar theories are acceptable provided the intended applications fall within the data base of the empirical modifications. However, extrapolation beyond the data base can only be made confidently with a method which predicts curvature effects naturally.

Since the mixing-length concept is entirely empirical, mixing-length models unsurprisingly require empirical curvature modifications. To make progress toward developing a theory which naturally predicts effects of curvature, less-empirical models must be used. Two-equation turbulence closure models<sup>5,9</sup> involve less empiricism than mixing length as evidenced by these models' ability to naturally predict effects of complicated phenomena, such as transition<sup>5,9</sup> and surface roughness,<sup>8,9</sup> effects which can only be treated empirically with mixing length. An obvious question is whether two-equation models also account for streamline curvature in a natural manner. The generally accepted notion is that they do not; computations such as those performed by Govindaraju<sup>10</sup> and Baldwin, et al.,<sup>11</sup> are usually offered to support this notion. Both researchers report poor agreement between computed and measured flow properties for the turbulent vortex, Govindaraju using the Saffman<sup>8</sup> turbulence model, and Baldwin, et al, using the Jones-Launders<sup>5</sup> model. Baldwin, et al, obtain improved agreement with experiment by introducing a streamline curvature correction term into the turbulent-energy equation; however, the term involves an empirical constant.

The purpose of this paper is to explain the results obtained in these early attempts and to show that, with proper consideration of the physics of turbulent flow with streamline curvature, two-equation models naturally predict flows with streamline curvature and coordinate-system rotation. Section II discusses our theoretical approach to modeling curved-streamline turbulent flows; physical reasoning is combined with singular perturbation methods to devise, without empiricism, curvature modification terms for the turbulent mixing-energy equation. Section III presents results of numerical solutions for several boundary layers on curved surfaces and for rotating channel flow.

## II. Theoretical Formulation

The model equations which form the basis of this study are summarized in this section. Physical meanings are given for the turbulent mixing energy and the turbulent dissipation rate, the two quantities needed to compute the eddy viscosity.

Presented as Paper 76-353 at the AIAA 9th Fluid and Plasma Dynamics Conference, San Diego, Calif., July 14-16, 1976; submitted Sept. 27, 1976; revision received Dec. 27, 1976.

Index category: Boundary Layers and Convective Heat Transfer-Turbulent.

\*President, Associate Fellow AIAA.

†Associate Engineer.

Physical aspects of streamline curvature and its effect upon turbulence structure near solid boundaries are then discussed; reasons are offered for failure of two-equation models in prior curved-streamline applications. Next, a curvature modification term is proposed for the turbulent mixing-energy equation; perturbation methods are used to demonstrate validity of the curvature term.

### Equations of Motion

The two-equation turbulence model developed by Wilcox and Traci<sup>9</sup> serves as the basis of our study of streamline curvature and coordinate-system rotation. For incompressible boundary layers on plane surfaces, the model equations are:

continuity

$$\frac{\partial u}{\partial x} + \frac{\partial v}{\partial y} = 0 \quad (1)$$

momentum

$$u \frac{\partial u}{\partial x} + v \frac{\partial u}{\partial y} = U_e \frac{dU_e}{dx} + \frac{\partial}{\partial y} \left[ (\nu + \epsilon) \frac{\partial u}{\partial y} \right] \quad (2)$$

turbulent mixing energy

$$u \frac{\partial e}{\partial x} + v \frac{\partial e}{\partial y} = \left[ \alpha^* \left| \frac{\partial u}{\partial y} \right| - \beta^* \omega \right] e + \frac{\partial}{\partial y} \left[ (\nu + \sigma^* \epsilon) \frac{\partial e}{\partial y} \right] \quad (3)$$

turbulent dissipation rate

$$u \frac{\partial \omega^2}{\partial x} + v \frac{\partial \omega^2}{\partial y} = \left\{ \alpha \left| \frac{\partial u}{\partial y} \right| - \left[ \beta + 2\sigma \left( \frac{\partial \ell}{\partial y} \right)^2 \right] \omega \right\} \omega^2 + \frac{\partial}{\partial y} \left[ (\nu + \sigma \epsilon) \frac{\partial \omega^2}{\partial y} \right] \quad (4)$$

where  $u$  and  $v$  are velocity components in the streamwise,  $x$ , and surface-normal,  $y$ , directions, respectively;  $U_e$  is the boundary-layer-edge velocity;  $\nu$  is kinematic viscosity and the eddy diffusivity,  $\epsilon$ , is the ratio of turbulent mixing energy,  $e$ , to turbulent dissipation rate,  $\omega$ , i.e.,

$$\epsilon = e/\omega \quad (5)$$

The quantity  $\ell$  is the turbulent length scale defined by

$$\ell = e^{1/2}/\omega \quad (6)$$

Values for the six closure coefficients  $\alpha$ ,  $\alpha^*$ ,  $\beta$ ,  $\beta^*$ ,  $\sigma$  and  $\sigma^*$  have been established from arguments based on widely observed properties of turbulent flows; their respective values are

$$\begin{aligned} \beta &= \frac{3}{20} & \beta^* &= \frac{9}{100} \\ \sigma &= \frac{1}{2} & \sigma^* &= \frac{1}{2} \\ \alpha &= \frac{1}{3} \left[ 1 - \frac{10}{11} \exp(-2Re_T) \right] & (7) \\ \alpha^* &= \frac{3}{10} \left[ 1 - \frac{10}{11} \exp(-Re_T/2) \right] \end{aligned}$$

where  $Re_T$  is turbulent Reynolds number, viz,

$$Re_T = e^{1/2} \ell / \nu \quad (8)$$

Physical meanings of turbulent mixing energy and dissipation rate have been discussed by Wilcox and Traci. For boundary layers,  $e$  and  $\omega$  are given by

$$e = \frac{9}{4} \langle v'^2 \rangle \quad (9)$$

$$\omega = \frac{3\nu}{\beta^*} \frac{\langle (\partial v'/\partial y)^2 \rangle}{\langle v'^2 \rangle} \quad (10)$$

where  $\langle \rangle$  denotes time average and  $v'$  is the surface-normal, fluctuating component of the velocity vector. As will be shown later, streamline curvature and coordinate-system rotation primarily affect the equation for the turbulent mixing energy, while the  $\omega$  equation appears to be unaffected by curvature and rotation. Because  $e$  and  $\omega$  occupy such a central position in curvature/rotation physics, we pause and review the physical interpretation of Eqs. (9) and (10).

### Physical Meaning of $e$ and $\omega$

To motivate the given definition of  $e$  note that, in analogy to the kinetic theory of gases, we write the eddy diffusivity as the product of a mixing velocity,  $v_m$ , and a mixing length,  $\ell_m$ , i.e.,

$$\epsilon = v_m \ell_m \quad (11)$$

The mixing velocity is characteristic of the average velocity with which fluid particles fluctuate normal to the plane of shear (note that this paper focuses upon thin shear layers for which shear planes are parallel to the surface). Similarly, the mixing length is characteristic of the distance a fluid particle travels during the fluctuation. Note that in kinetic theory,  $v_m$  is proportional to the sound speed and  $\ell_m$  is the mean free path. Combining Eqs. (5) and (6), and comparing the resulting expression with Eq. (11), we conclude that

$$v_m = e^{1/2}, \quad \ell_m = \ell \quad (12)$$

The first of Equations (12) implies that  $e$  is proportional to the kinetic energy of the fluctuating motion normal to the shear plane. Commonly, in two equation turbulence models  $e$  is regarded as the total kinetic energy of the turbulence,  $q^2/2$ , where

$$q^2 = \langle u'^2 \rangle + \langle v'^2 \rangle + \langle w'^2 \rangle \quad (13)$$

with  $u'$  and  $w'$  denoting the fluctuating velocity components in the streamwise and lateral directions, respectively. Defining  $e$  to be  $q^2/2$  is physically realistic only if the kinetic energy of

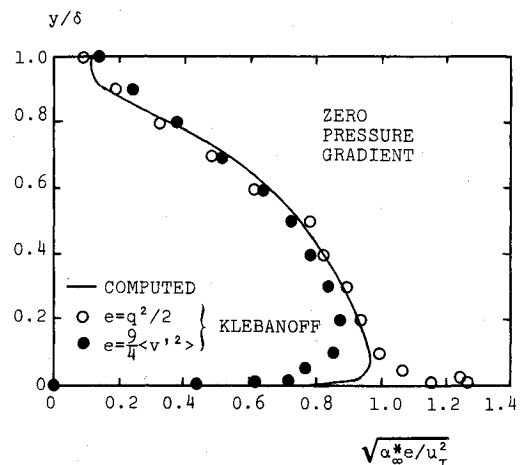


Fig. 1 Comparison of computed mixing energy with rms velocity fluctuation data; zero pressure gradient.

the turbulence is equipartitioned, i.e., only if the turbulence is isotropic (in which case  $q^2 = 3\langle v'^2 \rangle$ ). However, boundary-layer turbulence is anisotropic so that, more appropriately,  $e$  is proportional to  $\langle v'^2 \rangle$ . To establish the proportionality coefficient of  $9/4$  in Eq. (9), Wilcox and Traci insist that  $e$  be numerically equal to  $q^2/2$  in the law-of-the-wall region (wall layer) of a flat-plate boundary layer. The value  $9/4$  follows from the widely observed fact that  $q^2/2 \approx 9/4\langle v'^2 \rangle$  in the wall layer.

To substantiate the definition of  $e$  given in Eq. (9), Figs. 1 and 2 compare computed  $e$  profiles with experimental data for boundary layers with zero and adverse pressure gradients (note that  $\delta$  and  $u_\tau$  denote boundary-layer thickness and friction velocity, respectively). For the zero-pressure-gradient case, the computed  $e$  profile lies as close to Klebanoff's<sup>12</sup> measured  $9/4\langle v'^2 \rangle$  profile as it does to his measured  $q^2/2$  profile. However, close to the surface, the computed variation of  $e$  with  $y$  more nearly resembles that of  $9/4\langle v'^2 \rangle$ . Both the computed  $e$  and the measured  $9/4\langle v'^2 \rangle$  profiles tend to zero monotonically; by contrast, the  $q^2/2$  profile exhibits a sharp peak in the sublayer. Comparing computed values of  $e$  with Bradshaw's<sup>13</sup> data for a boundary layer subjected to an adverse pressure gradient is even more convincing. As shown in Fig. 2, the predicted  $e$  profile virtually duplicates the measured  $9/4\langle v'^2 \rangle$  profile through most of the boundary layer; measured  $q^2/2$  is generally 25% larger than predicted  $e$ .

Less is known regarding the physical meaning of  $\omega$ . It appears to be the rate at which  $\langle v'^2 \rangle$  kinetic energy is dissipated into heat, mean kinetic energy, and other fluctuation modes. The definition given in Eq. (10) is introduced by Wilcox<sup>14</sup> and generalized by Wilcox and Traci.<sup>9</sup> To establish Eq. (10) Wilcox notes that, for flow very close to a plane surface, the mixing-energy equation simplifies to

$$0 = -\beta^* \omega e + \nu \frac{\partial^2 e}{\partial y^2} \quad (14)$$

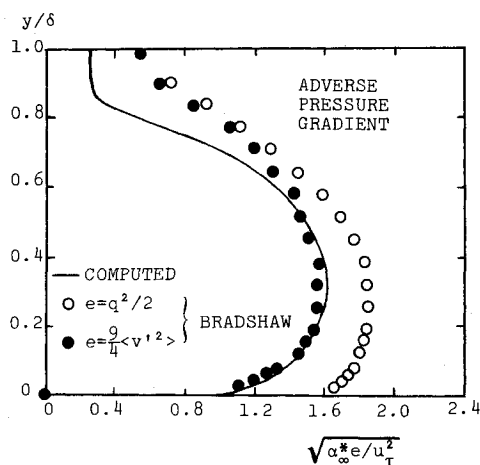


Fig. 2 Comparison of computed mixing energy with rms velocity fluctuation data; adverse pressure gradient.

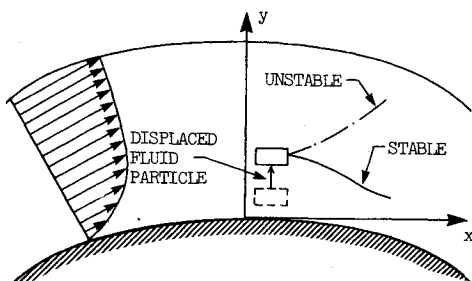


Fig. 3 Boundary-layer flow over a curved surface.

In the same limit, the exact equation for  $\langle v'^2 \rangle$  is

$$0 = - \left[ 3\nu \frac{(\partial \langle v'^2 \rangle / \partial y)^2}{\langle v'^2 \rangle} \right] \langle v'^2 \rangle + \nu \frac{\partial^2 \langle v'^2 \rangle}{\partial y^2} \quad (15)$$

Comparison of Eqs. (14) and (15) leads Wilcox to propose Eq. (10) as the definition of  $\omega$ . Wilcox and Traci generalize the definition by specifying  $y$  as distance normal to the plane of shear.

#### Curvature and Turbulence Physics

We turn now to discussion of the manner in which streamline curvature affects turbulent boundary layers. In order to recognize some important facets of curved-streamline flow, consider the classical stability arguments for flow over a curved wall (Fig. 3) advanced by von Karman.<sup>15</sup> Integral to his analysis is the behavior of a fluid particle perturbed in the direction normal to the wall. For incompressible flow, von Karman shows that if a fluid particle is displaced outwards and then released, it returns to its original position, provided the angular momentum of the mean flow increases outward: the flow is then said to be stable. If angular momentum decreases outward, the restoring force is insufficient to return the fluid particle to its original position and the particle continues an outward motion, which is termed unstable. Hence, according to von Karman, stability of a curved-wall boundary layer depends mainly on behavior of vertically moving fluid particles and not on any attendant nonvertical fluctuations. Von Karman's analysis thus suggests that, in a turbulent boundary layer, velocity fluctuations normal to the wall,  $\langle v'^2 \rangle$ , play an important role in streamline-curvature phenomenology.

The way in which curvature preferentially affects  $\langle v'^2 \rangle$  is further illustrated by examining the exact normal Reynolds stress equations for flow over a curved surface having a radius of curvature,  $R$ .

$$\frac{d}{dt} \langle u'^2 \rangle - 2\tau \frac{u}{R} = 2\tau \frac{\partial u}{\partial y} + \dots \quad (16)$$

$$\frac{d}{dt} \langle v'^2 \rangle + 2\tau \frac{u}{R} = -2\tau \frac{u}{R} + \dots \quad (17)$$

$$\frac{d}{dt} \langle w'^2 \rangle = \dots \quad (18)$$

where  $\tau = -\langle u'v' \rangle$  and  $d/dt = \partial/\partial t + u \cdot \nabla$ . The terms proportional to  $R^{-1}$  have two sources. Those on the left-hand sides of Eqs. (16) and (17) originate from the Coriolis and centrifugal accelerations attending flow about the curved surface. Those on the right-hand sides stem from the production term in the exact Reynolds-stress equation. Summing Eqs. (16-18) yields an equation for  $q^2/2$ .

$$\frac{d}{dt} (q^2/2) = \tau \left( \frac{\partial u}{\partial y} - \frac{u}{R} \right) + \dots \quad (19)$$

Inspection of Eqs. (16-18) shows that, for flow over a convex surface ( $R < 0$ ), the extra curvature terms tend to decrease  $\langle v'^2 \rangle$ , increase  $\langle u'^2 \rangle$ , and leave  $\langle w'^2 \rangle$  unaffected. Upon summation, the terms originating from Coriolis and centrifugal accelerations cancel identically, leaving only a minor curvature effect in the equation for  $q^2/2$ . Hence, convex curvature transfers kinetic energy from the normal to the streamwise direction in a manner which leaves the total kinetic energy of the turbulence relatively unaffected. Similarly, concave curvature transfers kinetic energy from the streamwise to the normal direction with a similar near invariance of  $q^2/2$ . The centrifugal term in the  $\langle v'^2 \rangle$  equation thus tends to suppress mixing over a convex wall ( $R > 0$ ) and to enhance mixing over a concave wall ( $R < 0$ ).

The notion of suppressed/enhanced mixing for flow over convex/concave walls is consistent with the observed decrease/increase of skin friction and heat transfer.

As shown by Wilcox and Chambers,<sup>16</sup> So,<sup>17</sup> and Mellor,<sup>18</sup> there is a more formal mathematical way of demonstrating that  $\langle v'^2 \rangle^{1/2}$  is the appropriate velocity scale for flow over curved surfaces. Specifically, starting with the Reynolds stress equation, and incorporating a Rotta-type distribution of energy hypothesis and assuming Kolmogorov-type isotropic dissipation (see Mellor<sup>18</sup> for more complete details), the shear stress is given in terms of present notation by

$$\tau \doteq \frac{9}{4} \frac{\langle v'^2 \rangle}{\omega} \frac{\partial u}{\partial y} \quad (20)$$

in the wall layer. Because we have assumed  $\tau = \epsilon \partial u / \partial y$  [cf Eq. (2)], comparison of Eqs. (5) and (20) illustrates consistency with the definition of  $e$  given in Eq. (9).

An explanation for the poor results obtained by Govindaraju and by Baldwin, et al, is now evident. Both investigators regard  $e$  as a scalar quantity which satisfies a scalar equation. The only way in which streamline curvature effects manifest themselves in a scalar equation is through the production terms where, in the context of flow over a curved surface,  $(\partial u / \partial y)$  is replaced by  $(\partial u / \partial y - u/R)$ . As with the turbulent kinetic energy equation [Eq. (19)], no effects of centrifugal acceleration appear in a scalar equation. In accord with the previous discussion, Govindaraju and Baldwin, et al, thus verify that such a minor modification to the  $e$  equation is insufficient to account for observed large effects of streamline curvature. Hence, the inaccurate predictions made by both investigators result from failure to account for effects of curvature on the mixing energy.

#### Revision of the Mixing Energy Equation

To account for effects of centrifugal acceleration on the mixing energy, we note two important points. First,  $e$  actually is proportional to one component of a second-rank tensor, i.e., the  $\langle v'^2 \rangle$  component of the Reynolds stress tensor. Second, the centrifugal acceleration term on the left-hand side of Eq. (17) arises because of the tensor transformation properties of the Reynolds stress equation. In light of these two facts, we can endow the tensor transformation properties of the Reynolds stress equation on the  $e$  equation by combining Eqs. (9) and (17). Also, assuming curvature changes  $\partial v' / \partial y$  and  $v'$  by comparable amounts, the definition of  $\omega$  [Eq. (10)] implies that the  $\omega$  equation truly is a scalar equation. We thus propose the following equations for *boundary layers on curved surfaces*:

$$u \frac{\partial e}{\partial x} + v \frac{\partial e}{\partial y} + \frac{9}{2} \frac{u}{R} \epsilon \frac{\partial u}{\partial y} = \left[ \alpha^* \left| \frac{\partial u}{\partial y} - \frac{u}{R} \right| - \beta^* \omega \right] e + \frac{\partial}{\partial y} \left[ (\nu + \sigma^* \epsilon) \frac{\partial e}{\partial y} \right] \quad (21)$$

$$u \frac{\partial \omega^2}{\partial x} + v \frac{\partial \omega^2}{\partial y} = \left\{ \alpha \left| \frac{\partial u}{\partial y} - \frac{u}{R} \right| - \left[ \beta + 2\sigma \left( \frac{\partial \ell}{\partial y} \right)^2 \right] \omega \right\} \omega^2 + \frac{\partial}{\partial y} \left[ (\nu + \sigma \epsilon) \frac{\partial \omega^2}{\partial y} \right] \quad (22)$$

The last term on the left-hand side of Eq. (21) is the curvature correction term. Note that the term's coefficient 9/2 follows directly from the definition of  $e$ . We have thus introduced a *nonempirical* modification which follows directly from careful interpretation of the physics of curved-streamline flows.

For flow in a coordinate system rotating at angular velocity  $\Omega$  normal to the flow plane, similar reasoning shows that

accounting for the Coriolis acceleration leads to the following form of the  $\langle v'^2 \rangle$  equation:

$$\frac{d \langle v'^2 \rangle}{dt} - 4\Omega \tau = \dots \quad (23)$$

Assuming the  $\omega$  equation is invariant under coordinate-system rotation, we thus propose the following equations for *boundary layers in a rotating coordinate frame*:

$$u \frac{\partial e}{\partial x} + v \frac{\partial e}{\partial y} - 9\Omega \epsilon \frac{\partial u}{\partial y} = \left[ \alpha^* \left| \frac{\partial u}{\partial y} \right| - \beta^* \omega \right] e + \frac{\partial}{\partial y} \left[ (\nu + \sigma^* \epsilon) \frac{\partial e}{\partial y} \right] \quad (24)$$

$$u \frac{\partial \omega^2}{\partial x} + v \frac{\partial \omega^2}{\partial y} = \left\{ \alpha \left| \frac{\partial u}{\partial y} \right| - \left[ \beta + 2\sigma \left( \frac{\partial \ell}{\partial y} \right)^2 \right] \omega \right\} \omega^2 + \frac{\partial}{\partial y} \left[ (\nu + \sigma \epsilon) \frac{\partial \omega^2}{\partial y} \right] \quad (25)$$

For flows over curved surfaces in a rotating coordinate system such as that existing in centrifugal impellers, Eqs. (21), (22), (24), and (25) are combined by subtracting the rotation term,  $9\Omega \epsilon \partial u / \partial y$ , from the left-hand side of Eq. (21). For simplicity in the present study, however, we consider curvature and rotation effects independently.

To provide a preliminary test of the curvature/rotation modification, we use perturbation methods to obtain model-predicted wall-layer solutions (i.e., solutions valid for  $u, y/\nu \gg 1$  and  $y/\delta \ll 1$ ). The objective of the perturbation analysis is to determine whether the model predicts the curved wall<sup>2</sup> and rotating-system<sup>4</sup> laws of the wall.

We first consider constant pressure flow over a curved boundary having radius of curvature  $R$ . The boundary layer thickness,  $\delta$ , is assumed to be very small relative to  $R$ . Additionally, the flow is assumed to have sufficiently high Reynolds number such that  $\phi \equiv |\nu/u, R| \ll 1$ . Analyzing model-predicted flow structure in the wall layer is very straightforward since convection and molecular effects are negligible; the wall-layer forms of the model equations are

$$\epsilon \left[ \frac{du}{dy} - \frac{u}{R} \right] = u_\tau^2 \quad (26)$$

$$\left[ \alpha_\infty^* \left| \frac{du}{dy} - \frac{u}{R} \right| - \beta^* \omega \right] e - \frac{9}{2} \frac{u}{R} \epsilon \frac{du}{dy} + \sigma^* \frac{d}{dy} \left[ \epsilon \frac{de}{dy} \right] = 0 \quad (27)$$

$$\left\{ \alpha_\infty \left| \frac{du}{dy} - \frac{u}{R} \right| - \left[ \beta + 2\sigma \left( \frac{d\ell}{dy} \right)^2 \right] \omega \right\} \omega^2 + \sigma \frac{d}{dy} \left[ \epsilon \frac{d\omega^2}{dy} \right] = 0 \quad (28)$$

where  $\alpha_\infty = 1/3$  and  $\alpha_\infty^* = 3/10$  are the limiting values of  $\alpha$  and  $\alpha^*$  for  $Re_\tau \rightarrow \infty$  [c.f., Eqs. (7)]. As can be easily verified, the perturbation solution to Eqs. (26-28) is [noting that the Karman constant  $\kappa = \sqrt{(\beta/\alpha_\infty^* - \alpha_\infty)/2\sigma}$ ] as follows:

$$\left[ 1 - \bar{\beta}_R \frac{y}{R} \right] \frac{u}{u_\tau} = \frac{1}{\kappa} \log \frac{u_\tau y}{\nu} + \dots \quad (29)$$

$$e = \frac{u_\tau^2}{\alpha_\infty^*} \left[ 1 - 6.23 \frac{u}{R} \log \frac{u_\tau y}{\nu} + \dots \right] \quad (30)$$

$$\omega = \frac{u_\tau}{\alpha_\infty^* \kappa y} \left[ 1 + 9.35 \frac{y}{R} \log \frac{u_\tau y}{\nu} + \dots \right] \quad (31)$$

where

$$\bar{\beta}_R = 16.6$$

This solution possesses two noteworthy features. First, Eq. (29) is identical to the modified law of the wall measured for

curved-wall boundary layers; the predicted value of  $\bar{\beta}_R$  is reasonably close to the value inferred from the Meroney-Bradshaw<sup>2</sup> measurements, viz,  $\bar{\beta}_R \approx 12$ . Second,  $e$  differs from its plane-wall value by order  $\nu/u_\tau R$ ; by contrast, the perturbation solution of the equation without the curvature modification indicates no change in  $e$  to order  $\nu/u_\tau R$ . The latter point further reinforces the fact that mixing energy is strongly affected by curvature while scalar quantities such as  $q^2/2$  are virtually unaffected.

We next turn to flow in a rotating channel. For simplicity we consider fully developed channel flow so that convective terms vanish identically. Then, neglecting molecular viscosity and expanding in powers of the Ekman number,  $\nu\Omega/u_\tau^2 < 1$ , there follows

$$\frac{u}{u_\tau} = \frac{1}{\kappa} \log \frac{u_\tau y}{\nu} - \bar{\beta}_C \left( \frac{2\Omega y}{u_\tau} \right) + \dots \quad (32)$$

$$e = \frac{u_\tau^2}{\alpha_\infty^*} \left[ 1 + 6.23\kappa \left( \frac{2\Omega y}{u_\tau} \right) + \dots \right] \quad (33)$$

$$\omega = \frac{u_\tau}{\alpha_\infty^* \kappa y} \left[ 1 - 9.35\kappa \left( \frac{2\Omega y}{u_\tau} \right) + \dots \right] \quad (34)$$

where

$$\bar{\beta}_C = 15.6$$

As with the curved-wall boundary-layer analysis, an altered law of the wall is predicted [Eq. (32)] which is consistent with experimental measurements. Specifically, Johnston<sup>19</sup> infers Eq. (32) from his measurements and states that " $\bar{\beta}_C \approx 6$  appears to be a good median value on the stable side, and on the unstable side of the channel." Although the predicted value of  $\bar{\beta}_C$  is larger than the value inferred by Johnston, note that Johnston's value is an average value for numerous measurements. As with the curved-wall boundary layer,  $e$  differs from its stationary-frame value by order  $\nu\Omega/u_\tau^2$ ; without the rotation term in the  $e$  equation,  $e$  is unaffected to all orders.

Results of the perturbation analysis substantiate the claim that curvature primarily affects the mixing energy. Also, the proposed curvature modifications appear to be responsible for the experimentally observed large effects of curvature on turbulent boundary layers. Results of the perturbation analysis are therefore very encouraging. Numerical computations of a variety of curved-streamline flows are needed to provide more definitive tests of the curvature modifications. We now consider numerical applications.

### III. Numerical Applications

This section presents results of numerical computations of boundary layers on curved surfaces and of rotating channel flow. Incompressible applications are discussed first. Then, supersonic flow over a cooled convex surface is analyzed. All computations have been performed with a second-order accurate, implicit boundary-layer code based on the method of Flugge-Lotz and Blottner.<sup>20</sup> Initial profiles are determined by the procedure discussed by Wilcox and Traci.<sup>9</sup> At the surface, boundary conditions suitable for a perfectly smooth

Table 1 Summary of incompressible calculations

Flow	Data source
Low-Reynolds-number turbulent flow past a cylinder	Patel <sup>21</sup>
Constant pressure flow over a convex wall	So-Mellor <sup>22</sup>
Separating flow over a convex wall	So-Mellor <sup>22</sup>
Rotating channel flow	Johnston <sup>23</sup>

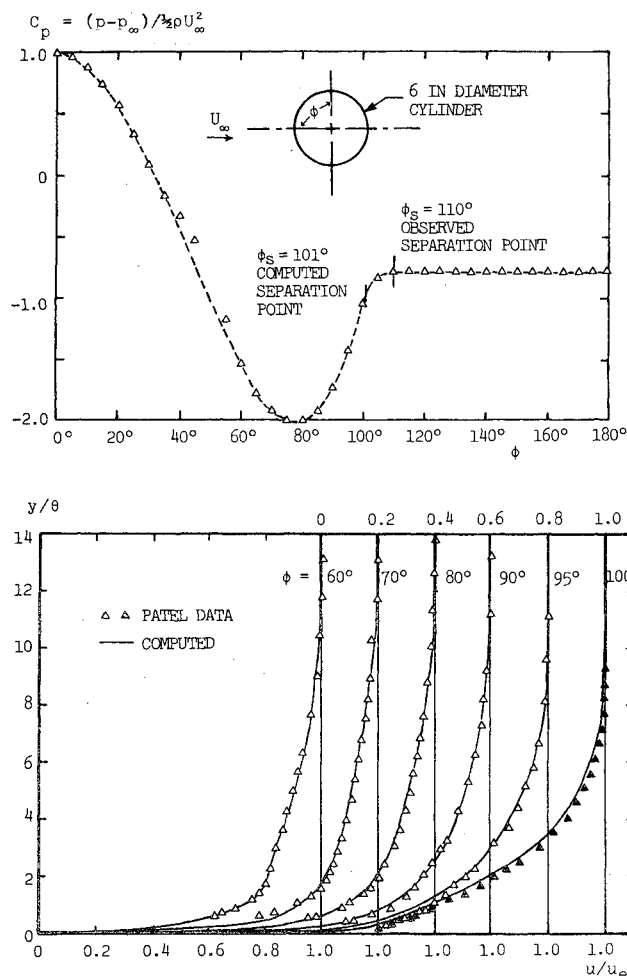


Fig. 4 Comparison of computed and measured flow properties for low-Reynolds-number turbulent flow past a cylinder;  $Re_D = 5.01 \cdot 10^5$ .

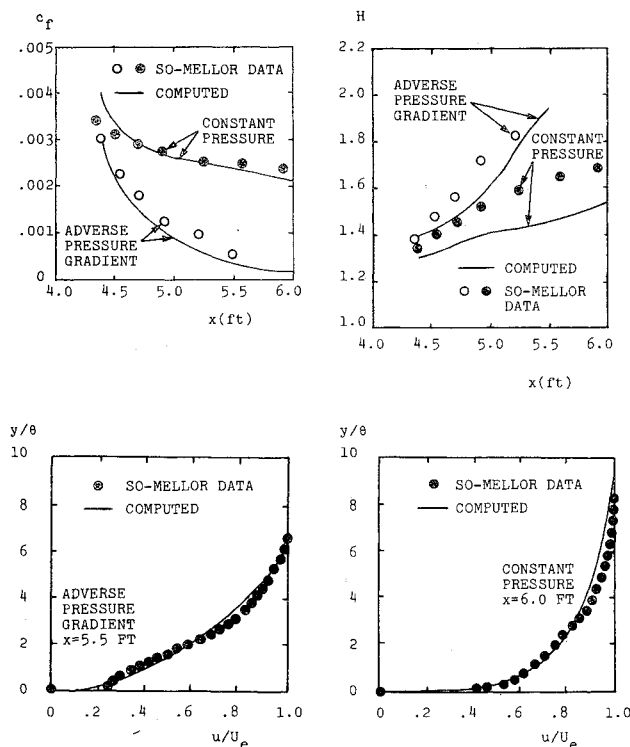


Fig. 5 Comparison of computed and measured flow properties for turbulent flow over a convex surface.

wall have been used, i.e.,

$$u=v=e=0, \quad y^2\omega=20\nu/\beta \text{ at } y=0 \quad (35)$$

At the boundary-layer edge, the values of  $u$ ,  $e$ , and  $\omega$  are prescribed from the following equations:

$$u=U_e, \quad e=iU_e^2, \quad \ell=.09\sqrt{\alpha_\infty^*}\delta \text{ at } y=\delta \quad (36)$$

where  $i \sim 4 \cdot 10^{-4}$ . Wilcox and Traci<sup>9</sup> present the rationale for these boundary conditions.

#### Incompressible Applications

Table 1 summarizes the incompressible applications; the table includes experimental data sources. Most difficult of all the incompressible cases considered is low-Reynolds-number turbulent flow past a cylinder. In addition to having streamline curvature and adverse pressure gradient, the flow is dominated by viscous phenomena. Figure 4 presents results of the computation. All computed quantities closely agree with experimental data of Patel.<sup>21</sup> The largest discrepancies between computed and measured velocity profiles are less than 10% throughout the flow. Even predicted and measured separation points are reasonably close; computed separation occurs at circumferential angle  $\phi = 101^\circ$  while Patel observes separation at  $\phi = 110^\circ$ . Additionally, computed shape factor and momentum-thickness Reynolds number differ from corresponding values by no more than 6%, even as the flow nears separation.

Figure 5 exhibits computed and measured flow properties for flow over a convex wall with constant pressure and with adverse pressure gradient. Computed and measured skin friction are within a few percent. In the separating flow, separation is observed between 5.50 and 5.83 feet downstream of the leading edge, while the computation indicates that separation occurs a little farther downstream. As can be seen from the figure, predicted shape factors show somewhat larger discrepancies from the measured values; the largest discrepancy is 12%. Finally, computed and measured velocity profiles differ by no more than 6%.

The final incompressible application is to rotating channel flow (Figs. 6 and 7). Velocity profiles with and without rotation are shown to illustrate the contrast between nonrotating and rotating channel velocity profiles. Also, Fig. 7 presents the ratio of rotating friction velocity,  $u_\tau$ , to nonrotating friction velocity,  $u_{\tau 0}$ , for a range of rotation numbers. Predictions are generally within 10% of corresponding measurements.

#### Compressible Application

To test the model's ability to predict curvature effects in a compressible flow, the model is now applied to Mach 2.5 flow over a cooled convex surface; the flow is experimentally documented by Thomann.<sup>3</sup> As shown by Wilcox and Traci,<sup>9</sup> the dependent variable  $w = \rho\omega$  must be used in place of  $\omega$  for compressible flows. Boundary-layer forms of the compressible model equations with curvature are as follows:

turbulent mixing energy

$$\begin{aligned} \rho\mu \frac{\partial e}{\partial x} + \rho\nu \frac{\partial e}{\partial y} + \frac{9}{2}\rho \frac{u}{R} \epsilon \frac{\partial u}{\partial y} = \left[ \alpha^*\rho \left| \frac{\partial u}{\partial y} - \frac{u}{R} \right| - \beta^*w \right] e \\ + \frac{\partial}{\partial y} \left[ (\mu + \sigma^*\rho\epsilon) \frac{\partial e}{\partial y} \right] \end{aligned} \quad (37)$$

turbulent dissipation rate

$$\begin{aligned} \rho\mu \frac{\partial w^2}{\partial x} + \rho\nu \frac{\partial w^2}{\partial y} = \left\{ \alpha\rho \left| \frac{\partial u}{\partial y} - \frac{u}{R} \right| - \left[ \beta + 2\sigma \left( \frac{\partial \ell}{\partial y} \right)^T \right] w \right\} w^2 \\ + \frac{\partial}{\partial y} \left[ (\mu + \sigma\rho\epsilon) \frac{\partial w^2}{\partial y} \right] \end{aligned} \quad (38)$$

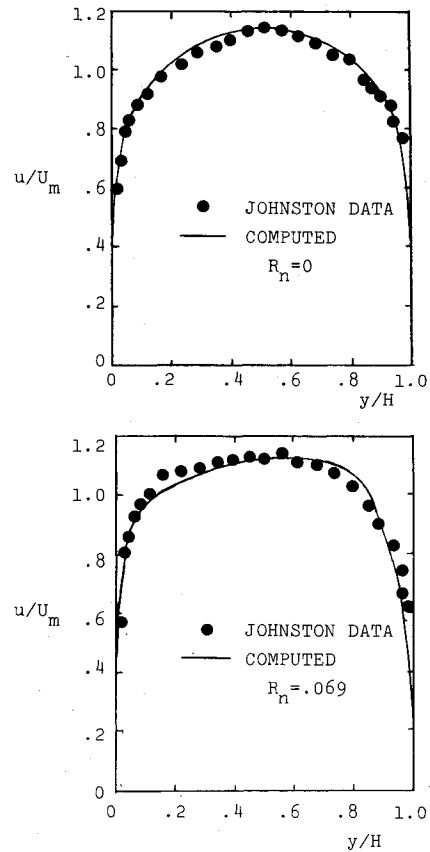


Fig. 6 Comparison between computed and measured flow properties for rotating channel flow;  $R_n = \Omega H/U_m$  where  $U_m$  is the average flow velocity and  $h$  is channel width;  $Re_H = U_m H/\nu$ .

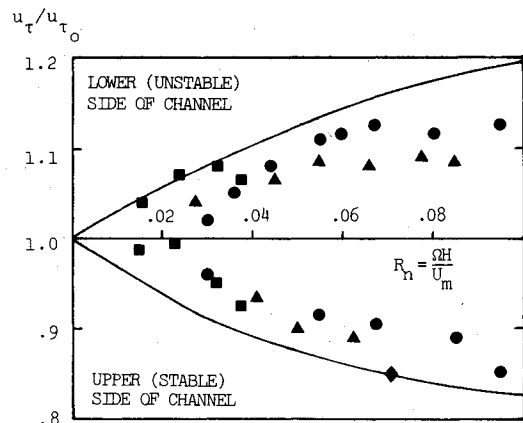


Fig. 7 Comparison of computed and measured values of  $u_\tau/u_{\tau 0}$  as a function of rotation number,  $R_n$ , for rotating channel flow; computed, —  $Re_H = 12000$ ; Johnston data,  $\diamond$   $Re_H = 11400$ ,  $\blacksquare$   $Re_H = 23400$ ,  $\bullet$   $Re_H = 25700$ ,  $\blacktriangle$   $Re_H = 33100$ .

where

$$\epsilon = \rho e/w; \quad \ell = \rho e^{1/2}/w \quad (39)$$

The quantities  $\rho$  and  $\mu$  denote density and molecular viscosity (given by Sutherland's law), respectively.

Figure 8 compares computed and measured Stanton number; for contrast, results are shown for both a plane wall and for a convex wall with  $\delta/R = .022$ . For the plane-wall, calculated values of  $S_t$  are within 6% of the Hopkins-Inouye<sup>24</sup> correlation and generally within 3% of Thomann's<sup>3</sup> data. As with the incompressible cases, the model predicts the strong stabilizing effect of convex curvature. Specifically, the measured  $S_t$  is 17% less than its plane-wall value at  $x = 1.4$

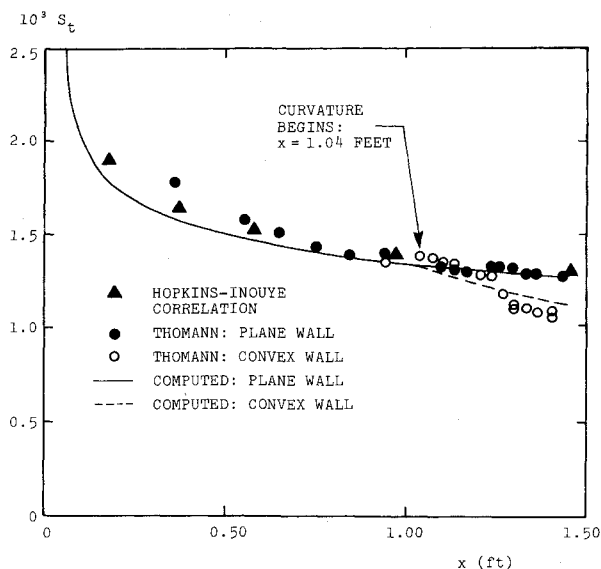


Fig. 8 Comparison of computed and measured Stanton number for Mach 2.5 flow over a cooled convex surface;  $T_w/T_{aw} = 0.78$ .

feet while the model predicts a 13% decrease. The model thus appears to predict effects of curvature accurately for both compressible and incompressible boundary layers.

#### IV. Discussion

Results of the perturbation analyses and the numerical applications show that, with the curvature/rotation modification terms devised in Sec. II, the Wilcox-Traci model accurately predicts effects of streamline curvature and coordinate-system rotation on turbulent boundary layers. Since the modification terms have been devised from nonempirical, physically based arguments, we have thus shown that the model predicts curvature/rotation effects in a natural manner. Consequently, the model probably encompasses an even wider class of curved-streamline rotating flows than those considered in Sec. III. The model can reasonably be expected to apply, in a two-dimensional computation, to any turbulent boundary-layer flow in which longitudinal vortices are not present. However, when such vortices appear, the mean flow is three-dimensional so that a two-dimensional calculation is inappropriate. Any comments pertaining to the model's applicability to such flows in a three-dimensional computation would be only speculative at this point.

One of the most important results of the present study is the physical interpretation of the fluid dynamical processes attending flow over curved boundaries. The key role played by  $\langle v'^2 \rangle$ , and the insensitivity of  $q^2/2$  in curved-streamline/rotating flows previously has not been quantified; the perturbation analyses of Sec. II are particularly illuminating in this respect. Explanations for the inaccurate turbulent-vortex computations of Govindaraju and Baldwin, et al, follow directly from consideration of the difference between behavior of  $\langle v'^2 \rangle$  and  $q^2/2$  when streamline curvature is pertinent.

Based on the success achieved in this study, further model testing and development is warranted. For example, more compressible applications are needed to test the model. Also, generalizing the curvature modification term for arbitrary coordinate systems would permit the model's application to separating flows; such applications would help determine the importance of local streamline curvature in the separation process.

#### Acknowledgment

Research sponsored by NASA Ames Research Center under Contracts NAS2-8884 and NAS2-9135. M.W. Rubesin of NASA Ames Research Center provided invaluable guidance during the study.

#### References

- Bradshaw, P., "Effects of Streamline Curvature on Turbulent Flow," AGARD-AG-169, 1973.
- Meroney, R.N. and Bradshaw, P., "Turbulent Boundary-Layer Growth Over a Longitudinally Curved Surface," *AIAA Journal*, Vol. 13, Nov. 1975, pp. 1448-1453.
- Thomann, H., "Effect of Streamwise Wall Curvature on Heat Transfer in a Turbulent Boundary Layer," *Journal of Fluid Mechanics*, Vol. 33, 1968, pp. 283-292.
- Eide, S.A. and Johnston, J.P., "Prediction of the Effects of Longitude Wall Curvature and System Rotation on Turbulent Boundary Layers," Dept. of Mech. Engr., Stanford University, Stanford, Calif., Rept. No. PD-19, 1974.
- Jones, W.P. and Launder, B.E., "The Prediction of Laminarization with a Two-Equation Model of Turbulence," *International Journal of Heat and Mass Transfer*, Vol. 15, 1972, pp. 301-314.
- Ng, K.E. and Spalding, D.B., "Turbulence Model for Boundary Layers near Walls," *Physics of Fluids*, Vol. 15, Jan. 1972, pp. 20-30.
- Launder, B.E. and Spalding, D.B., *Mathematical Models of Turbulence*, Academic Press, London, 1972.
- Saffman, P.G., "A Model for Inhomogeneous Turbulent Flow," *Proceedings of the Royal Society, London*, Vol. A317, 1970, pp. 417-433.
- Wilcox, D.C. and Traci, R.M., "A Complete Model of Turbulence," AIAA Paper 76-351, San Diego, Calif., 1976.
- Govindaraju, S.P., "A Study of Some Turbulent Flows Using a Model for Inhomogeneous Turbulence," PhD Thesis, Cal Tech, Pasadena, Calif., 1970.
- Baldwin, B.S., Chigier, N.A. and Scheaffer, Y.S., "Decay of Far Flow Field in Trailing Vortices," NASA TN D-7568, 1974.
- Klebanoff, P.S., "Characteristics of Turbulence in a Boundary Layer with Zero Pressure Gradient," NACA Report 1247, 1955.
- Bradshaw, P., "The Response of a Constant-Pressure Turbulent Boundary Layer to the Sudden Application of an Adverse Pressure Gradient," ARC R&M 3575, 1969.
- Wilcox, D.C., "Turbulence Model Transition Predictions: Effects of Surface Roughness and Pressure Gradient," AIAA Paper 75-857, Palo Alto, Calif., 1975.
- Von Karman, T., "Some Aspects of the Turbulence Problem," *Proceeding of the 4th International Congress of Applied Mechanics*, Cambridge, 1934, p. 54.
- Wilcox, D.C. and Chambers, T.L., "Streamline Curvature Effects on Turbulent Boundary Layers," DCW Industries, Sherman Oaks, Calif., Report DCW-R-04-01, 1975.
- So, R.M.C., "A Turbulence Velocity Scale for Curved Shear Flows," *Journal of Fluid Mechanics*, Vol. 70, 1975, pp. 37-57.
- Mellor, G.L., "A Comparative Study of Curved Flow and Density-Stratified Flow," *Journal of the Atmospheric Sciences*, Vol. 32, 1975, pp. 1278-1282.
- Johnston, J.P., "The Suppression of Shear Layer Turbulence in Rotating Systems," AGARD-CP-93, 1972, pp. 26.1-26.9.
- Flügge-Lotz, I. and Blottner, F.G., "Computation of the Compressible Laminar Boundary-Layer Flow Including Displacement-Thickness Interaction Using Finite-Difference Methods," Air Force Office of Scientific Research, Washington, D.C., AFOSR 2206, 1962.
- Patel, V.C., "The Effects of Curvature on the Turbulent Boundary Layer," Engineering Dept., Cambridge Univ., Cambridge, England, Reports and Memoranda No. 3599, 1968.
- So, R.M.C. and Mellor, G.L., "An Experimental Investigation of Turbulent Boundary Layers Along Curved Surfaces," Rept. NASA CR-1940, 1972.
- Johnston, J.P., Halleen, R.N., and Lezius, D.K., "Effects of Spanwise Rotation on the Structure of Two-Dimensional Fully Developed Turbulent Channel Flow," *Journal of Fluid Mechanics*, Vol. 56, Part 3, 1972, pp. 533-557.
- Hopkins, E.J. and Inouye, M., "An Evaluation of Theories for Predicting Turbulent Skin Friction and Heat Transfer on Flat Plates at Supersonic and Hypersonic Mach Numbers," *AIAA Journal*, Vol. 9, June 1971, pp. 993-1002.